

# Analyzing Green View Index and Green View Index best path using Google Street View and deep learning

Jiahao Zhang  
Osaka University  
zjhambition@gmail.com

Anqi Hu  
Osaka University  
anqihu1028@gmail.com

## Abstract

*As an important part of the urban landscape research, analysing and studying streetscape can increase the understanding of the cities' infrastructure, which contributes to better planning and design of the urban living environment. In this paper, we used Google Street View to obtain street view images of Osaka City. The semantic segmentation model is adopted to segment the Osaka City street view images and analyse the Green View Index (GVI). Based on the GVI value, we take advantage of adjacency matrix and Floyd algorithm is used to calculate Green View Index best path, solving the limitations of ArcGIS software. Our analysis not only allows the calculation of specific routes for the GVI best paths, but also realize the visualization and integration of neighbourhood landscape. By summarising all the data, a more specific and objective analysis of the landscape in the study area can be carried out, and based on this, the available natural resources can be maximized for a better life.*

## 1. Introduction

The urban streetscape is an important part of the urban landscape. The environmental resources that people live in possibly affect their lifestyle. Several studies have shown a positive relationship between the availability of the urban landscape and the health of inhabitants, which may provide opportunities for health improvement [1, 2]. It can also make some extent contributes to noise mitigation [3, 4]. In addition, streetscapes have a relationship to heat regulation in cities, like street, vegetation can reduce the heat island effect through shading and transpiration [5, 6]. Therefore, street greening is not only a significant presence for people in terms of aesthetics but also a convenient strategy for adaptive environmental design in urban life, creating thermally comfortable and more attractive living environments.

There are many evaluation indexes for the evaluation of street greening, among which the current research [7, 8]

is more widely focused on the Green View Index (GVI). The GVI can quantify the amount of greenery within the pedestrians' field of view and is more suitable for describing the environment observed by the human eye, which can partially compensate for the shortcomings of traditional assessment indexes [9]. With the development of science and technology, there has been a great progress from the collection of street view image to image processing [10, 11]. However, most studies stay at the level of collecting basic GVI data [12], focusing on how to use new technical tools to turn urban streetscapes into visual data charts to analyze the distribution characteristics of urban visual greenery, such as GVI maps, heat maps, etc. Therefore, there have some problems proposed: (1) how to take advantage of the GVI data after describing the greening degree; (2) how to use the data to build a more humanized and diversified street environment; (3) how to live better in the existing environment.

Therefore, we argue that designing an optimal GVI path not only makes use of the GVI data for the whole city, but provides a novel route of travel that maximises the use of the city's existing green landscape, enhances the overall impression of the city and improves the health of the inhabitants. The problem of computing the best path of GVI can be equated to the longest path problem, which in graph theory and theoretical computer science refers to finding the longest path of length in a given graph [13]. The length of a path in an unweighted graph is the number of edges, while the length of a path in a weighted graph is the sum of the edge weights. Unlike the shortest path problem, which can be solved in polynomial time, the longest path problem is NP-hard, meaning that unless  $P = NP$ , corresponding to an arbitrary graph, there is no way to solve the problem in polynomial time [13]. Thus, the longest path problem is a difficult and important problem. We tried to find the best GVI path by transforming the difficult and complex longest path problem into a shortest path problem by attempting different shortest path algorithms, such as Dijkstra's Algorithm, Floyd-Warshall Algorithm, Bellman-Ford Algorithm [14]. Finally we used the Floyd-Warshall Algorithm to find the best GVI path, which will be explained in detail in sec-

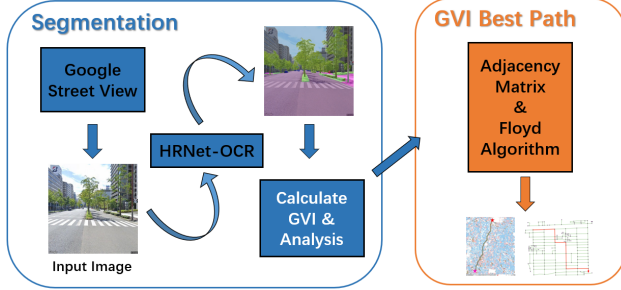


Figure 1. The total flowchart of proposed method.

tion 4.2.

In this paper, we aim to calculate the GVI data by street image analysis and use the GVI data to calculate the GVI best paths in city. The flowchart is shown in Fig.1.

(1) Firstly, the coordinates of all street network road intersections in Osaka City, were collected through the google open source API (application programming interface) as the investigation site for the study, with a total of 49770 nodes. In order to collect more comprehensive street view information, we set the width of view field to  $60^\circ$ , and selected one image at every 60 degrees to get a set of six images containing  $0^\circ$ ,  $60^\circ$ ,  $120^\circ$ ,  $180^\circ$ ,  $240^\circ$ , and  $300^\circ$ , which can cover 360-degree panoramic street view (see Fig.2). A total of 298,620 street view images of Osaka City were collected.

(2) The obtained images are segmented by image segmentation model HRNet-OCR [15]. The value of GVI, which is the ratio of green view index (vegetation and terrain) in the landscape elements of the street view image, was calculated to assess the degree of green view of the image.

(3) Create a map of the GVI distribution of Osaka City. The evaluation criterion about the GVI is referred to the survey report of the Ministry of Land, Infrastructure, Transport and Tourism of Japan<sup>1</sup> and the satisfaction criteria of the first phase of the Kyoto Greening Promotion Plan<sup>2</sup> about the GVI. The GVI was divided into four grades: 0~10%, 10~18%, 18~25%, and 25% or more. Based on this criterion, a general overview of GVI distribution and degree of satisfaction in Osaka City was constructed.

(4) We have adopted a common best GVI path approach that converts the best GVI path problem into a shortest path problem to deal with. Although the algorithm for the shortest path exists in ArcGIS, it does not calculate the best GVI path correctly in complex scenarios.

The following contributions were achieved: (1) Visualized statistics were compiled on the distribution of GVI in Osaka City. (2) We evaluate and visualize the satisfaction of GVI in Osaka City. (3) A generalized approach is pro-

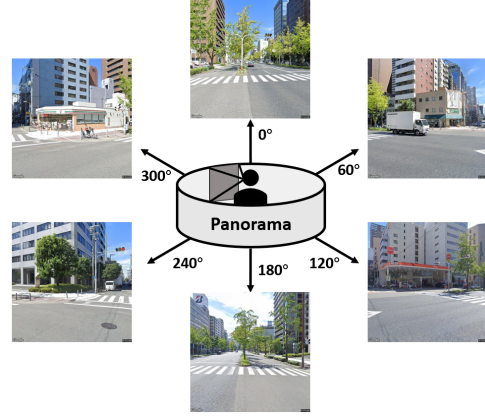


Figure 2. The example of obtaining a street view image from a panorama in this paper.

posed to implement the GVI best path in complex situations without using software and visualize it on a map with geographic data. (4) We adopted directional GVI values instead of using the average of each point to calculate the GVI, and compared the variability of the best GVI paths by both true and average values in an ideal area (Imazu Park) of due east, west, south, and north.

## 2. Related Works

### 2.1. Google Street View

Google Street View is an interactive web map that is highly accessible and has a wide coverage all over the world. It provides a  $360^\circ$  panoramic view of the city, capturing all scenes of a street or neighborhood. Street view shows the basic information of the landscape from the human perspective and offers considerable possibilities for urban visual greening studies. Street view image has now been used extensively in various researches [5, 16]. These studies have shown that street view image data sets are useful and quantitative tools to help policy makers, planners and researchers to understand the streetscape from the human perspective. In recent years, Google Maps<sup>3</sup> and Baidu Maps<sup>4</sup> have Provided Nodes of Interest (POI) alternatives in their public Geographic Information System (GIS) databases. With the development of these public GIS databases, easier access to raw data (street view image API) facilitates large scale street view image based research [5, 17].

### 2.2. Semantic Segmentation for GVI Analysis

In computer vision field, deep learning uses Deep Neural Networks [18] (DNN) for feature extraction and parameter optimization. Semantic segmentation is one of the branches

<sup>1</sup>[https://www.mlit.go.jp/kisha/kisha05/04/040812\\_3/01.pdf](https://www.mlit.go.jp/kisha/kisha05/04/040812_3/01.pdf)

<sup>2</sup><https://www.city.kyoto.lg.jp/kensetu/cmsfiles/contents/0000102/102008/planhonpen.pdf>

<sup>3</sup><https://www.google.com/streetview/>

<sup>4</sup><http://lbsyun.baidu.com/>

to classify each pixel in a image with different classes based on training data. It is a kind of supervised learning [19]. For natural images, it is achieved by using neural networks to identify landscape categories on pixel-level, rather than identifying their type and position in the overall image. There are many scenarios where semantic segmentation is currently used, for example, in civil engineering [20], to detect cracks in concrete; in medical field to identify diseases in X-ray images [21] and in autonomous driving for road boundary and object detection [22].

Models for semantic segmentation have developed rapidly in recent years, and representative models include U-Net [23], SegNet [24], DeepLabv3+ [25], PSPNet [19], and so on. All these models have shown good results in terms of a common evaluation metric intersection-over-union (IoU). In this study, We strongly refer to the official model benchmark rankings of pixel-level semantic labeling task of the Cityscape Dataset [26], and we decided to use HRNet [27] as the backbone and OCRNet as the semantic segmentation model, to analyze street view images and calculate GVI values.

A number of studies have been proposed using semantic segmentation to conduct analysis of urban green views and landscapes. [28] used Google Street View images at different times to map and analyze the spatial distribution and temporal variation of the GVI in New York City. [29] proposed an improved GVI method to analyze the main neighborhoods of Yokohama, Japan. Besides, there have existed many pioneering studies on the integration of landscape data processing with GIS research, such as [30] in which used geographic data analysis tools of ArcGIS to analyze and assess the accessibility of urban green spaces. In [31], aerial photographs were implemented on GIS for view area analysis. Three types of landscapes were quantified: open landscapes (visibility), green landscapes (visibility of open spaces), and marine landscapes (visibility of the ocean). It is shown that ArcGIS is a very useful tool in achieving the level of integration of photo information quantification and geographic data [31]. There has no research has been published to analyze GVI of Osaka City using an open source street view API, so we decided to fill this gap and perform a systematic GVI analysis of Osaka City.

### 2.3. The Researches of the Best GVI path

Many researches trend towards the development of new routing algorithms for finding routes with optimised exposure [32, 33]. [34] analysed the effect of GVI on runner satisfaction. [33] developed a software Green Paths using python toolkits to analyze paths in Helsinki under different exposure scenarios, such as traffic noise levels, air quality and street greenery. [35] proposed a system for generating customised pedestrian routes based entirely on OpenStreetMap (OSM) data. By selecting OSM features, tags

considered to be green features are extracted and the green areas are represented in the top view.

## 3. Material and Method in Deep Learning

In this study, we constructed a GVI distribution map system according to the following process: (1) Obtain the street view images of Osaka City. (2) Semantic segmentation of streetscape images with HRNet-OCR, with HRNet as the backbone and OCRNet as the semantic segmentation model. (3) Calculate the GVI of different directions and the average GVI for each node. (4) Integrate the geographic data with GIV data using ArcGIS to visualize the GVI value. (5) The GVI best path was calculated and visualized with geographic data by proposed method.

### 3.1. Research Area

We considered the entire city of Osaka as the study area, since we used it in order to verify that our proposed algorithm can calculate the best GVI path for any two points within the city of Osaka.

Osaka City in Japan is the administrative, economic, cultural and transportation center of the Kinki region and western Japan. It has an area of approximately 225.21 km<sup>2</sup> and is composed of 24 administrative districts. The Osaka Metropolitan Area and the Keihan-Kobe Metropolitan Area are formed with Osaka City as the center. The Keihan-Kobe Metropolitan Area is second only to the Tokyo Metropolitan Area in terms of Gross Domestic Product (GDP) in Japan and ranks among the highest in the world. It was ranked 35<sup>th</sup> in the world in the "Global Cities Index 2020" ranking of world cities by a U.S. think tank<sup>5</sup>. It is well suited as a target city for conducting researches of urban landscapes. Therefore, we set Osaka City as first target area to calculate and visualize GVI distribution as a way to understand the city overall. The visualization of the distribution facilitates a more intuitive understanding.

In the section of GVI best path, it is impractical to analyse GVI path of all Osaka City because we could not get street view facing the road at the intersection in Osaka City by Google Map APIs. So in order to verify whether the methods of getting the best GVI path are feasible, we select a representative area in Osaka City where at each intersection, it is possible to get an ideal angle of view facing due east, west, north and south, i.e. the direction of view is parallel to the road. Therefore we set Imazu Park and its surrounding area (see Fig.3) as the second target area to analyse detailed GVI best path.

### 3.2. Get Street View Images of Osaka City

In order to get map networks of Osaka City, we used the Python OSMnx package [36] to obtain the coordinate

<sup>5</sup><https://www.kearney.com/global-cities/2020>

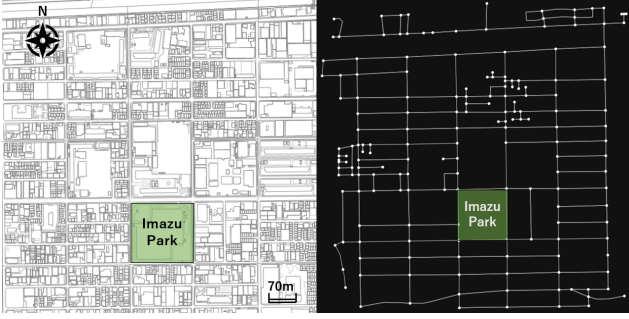


Figure 3. The diagram of Imazu Park and surrounding area.

data of all intersections in Osaka City from the Open Street Map. With the overall networks, we can get coordinates of all the intersections. In recent years, companies such as Google, Amazon, and Twitter have been actively providing data through web service APIs for the purpose of leveraging the various types of big data they have. Google Street View Image API makes it easy to download Google Street View images. Therefore, we collected street view images by Google Map API with obtained coordinates of all intersections in Osaka City (a total of 49770 nodes). Street view images were collected for six angles ( $0^\circ$ ,  $60^\circ$ ,  $120^\circ$ ,  $180^\circ$ ,  $240^\circ$ ,  $300^\circ$ ) in the direction of the street centered at each intersection. The size of them was  $640 \times 640$ , because by Google Map API we can only get the maximum size of  $640 \times 640$ . In order to get more accurate result by HRNet-OCR, we need as much as possible to get high resolution of input image. We totally download 298,620 images of Osaka City. One thing need to be mentioned, the street view images obtained may not be suitable for analysis, such as night-time street scenes, indoor images and blurred images. These nodes need to be manually filtered and discarded.

### 3.3. Semantic Segmentation and Calculate GVI

In this study, we use HRNet-OCR as basic model for GVI extraction which was pre-trained on Cityscapes [26] to generate segmented images into 19 landscape elements. The motivation of choosing such method for semantic segmentation is that the HRNet has meaningful semantic features as well as OCR method is to explicitly transform the pixel classification problem into an object region classification problem [37]. Semantic segmentation is location-sensitive in computer vision domain tasks, and maintaining a high-resolution feature map is a simple and effective way to process the model in order to make the task location information more accurate. But in fact almost all networks before HRNet did the same way, by downsampling to get stronger semantic information, and then upsampling to recover high resolution recovered position information. However, the approach will lead to a large amount of valid information lost in the process of constant upsampling and downsampling. HRNet, on the other hand, achieves both

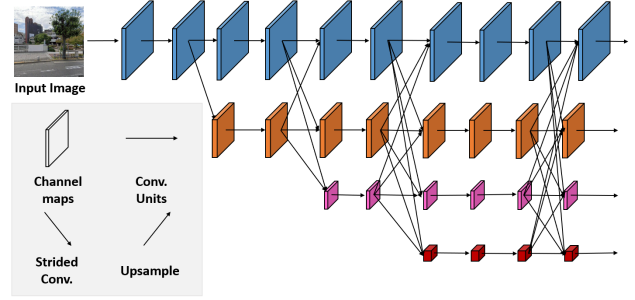


Figure 4. The basic structure of HRNet backbone.

strong semantic information and accurate location information by parallelizing multiple branches of resolution, coupled with constant interaction of information between different branches [27]. The basic structure of HRNet backbone is shown in Fig.4.

The main idea of OCR is consistent with the original definition of the semantic segmentation problem, i.e. the class of each pixel is the class of the object to which the pixel belongs, in other words, the main difference with the contextual information of PSPNet and DeepLabv3+ is that the OCR method explicitly enhances the object information. The pipeline of OCRNet is shown in Fig.5. The pixel representation is the feature map output by HRNet, where each node in feature map contains a pixel feature at corresponding location. In Cityscapes Dataset, the soft object regions below contain 19 different classes of features, with a different position in each class indicating the probability that the feature at certain location belongs to corresponding class [15]. The pixel representation is dotted with the soft object regions to obtain object region representations, which represent the feature representation of the region corresponding to each category. The dot product of pixel representation and object region representations yields pixel-region relations. The weighted sum of the pixel-region relations and the object region representations are used to generate object contextual representations, where concatenated with the HRNet output feature map to obtain the final augmented representation containing rich semantic features [15]. The overall view is that OCRNet uses the Transformer [38] as the basic idea to integrate features through a self-attention mechanism.

For the training process, we download labeled open source data set Cityscapes which contains 5,000 images with correlated fine label in Europe. The entire data set is divided into three parts, 75% of them is for training, 10% for validation and 15% for test. Even though the basic composition and details are different, for the composition on class level, we can get clear segmentation result by HRNet-OCR which is pre-trained on Cityscapes. The colored label image is transformed to true label image which use index of class as pixel number in order to improve training efficiency.



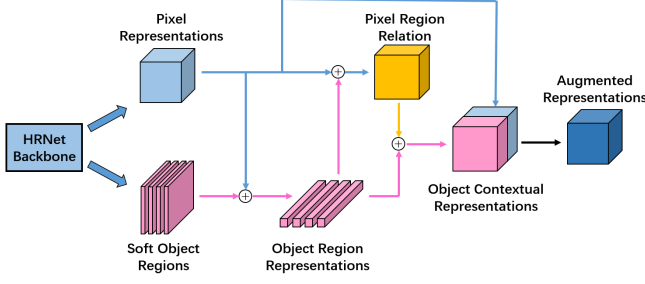


Figure 5. The pipeline of OCRNet [37].

Because the original training data has large image size, we also need to set crop window with relatively small size on local part of original image, ensuring not to lose much basic information if we straight resize the original image in training data set. For the evaluation criterion of training result, we use intersection-over-union to evaluate the result of segmentation. It is consisted of three part, for each class, the generated region of one class is calculated by IoU with label region. The IoU is defined as below:

$$IoU = \frac{TP}{TP + FP + FN} \quad (1)$$

where  $TP$  is True Positive,  $FP$  is False Positive and  $FN$  means False Negative. This criterion can be simplified by the ratio of intersection area of each class between generated region and label region to the union area between them. The mean IoU of HRNet-OCR achieved 80.6% in our test set. The inference result of Osaka City is shown in Fig. 6. In fact, the size of the generated segmented image is closely related to the generation efficiency. As Osaka City contains a large number of images, we have reduced the generated image size from  $2048 \times 1024$  to the original image size, which is  $640 \times 640$ , in order to improve the inference efficiency of segmentation. We spent almost 90 hours to generate segmented street view images of Osaka City. In order to calculate ratio of greenery in a whole street view image, we need to select vegetation and terrain as target colors to calculate GVI value.

In a segmented image, for each angle  $i \in (0^\circ, 60^\circ, 120^\circ, 180^\circ, 240^\circ)$ ,  $G_i$  is the number of greenery pixels.  $T_i$  means the total number of this segmented image.  $GVI_i \in \{0, 1\}$  means corresponding GVI value of this angle, which is given by

$$GVI_i = \frac{G_i}{T_i} \times 100\% \quad (2)$$

For each intersection node  $M$ , which contains number of  $m$  street view images. The average of  $GVI_i$  represents GVI value of this node. Therefore, the  $GVI_{avg}$  of each intersection is given by

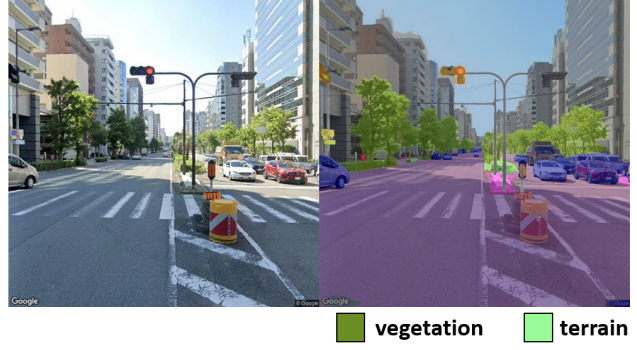


Figure 6. Inference example of street view of Osaka City and its corresponding labels (vegetation and terrain).

$$GVI_{avg} = \frac{1}{m} \sum_{i=1}^m GVI_i \times 100\% \quad (3)$$

where  $m = 6$  in this paper.

### 3.4. Integration and Visualisation of GVI data

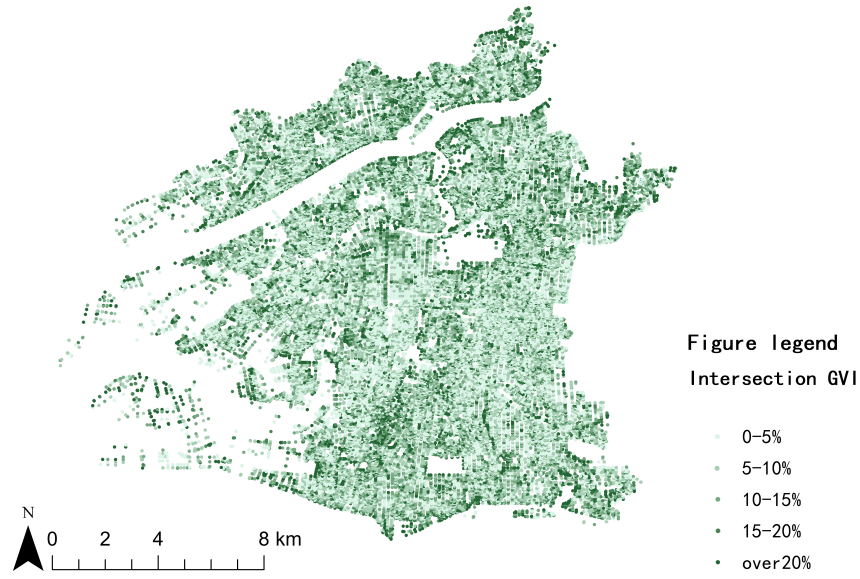
After getting the geographic data included street line and node network by open street map, we can also get an excel with GVI data and coordinate. In order to make node and line map to visualize the GVI distribution in Osaka City, we use ArcGIS to integrate them manually. The created node map of the distribution of GVI value in Osaka City is shown in Fig. 7(a). Each node is represented by  $GVI_{avg}$  and its coordinate with various color depths in five classes.

In order to get GVI value of streets in Osaka City to represent GVI line map, based on GVI node map, we have adopted a criterion that uses the average of the GVI values of the vertices on both sides of the street to represent the value of the overall street. Therefore, the line map of GVI distribution in Osaka City was obtained as shown in Fig. 7(b).

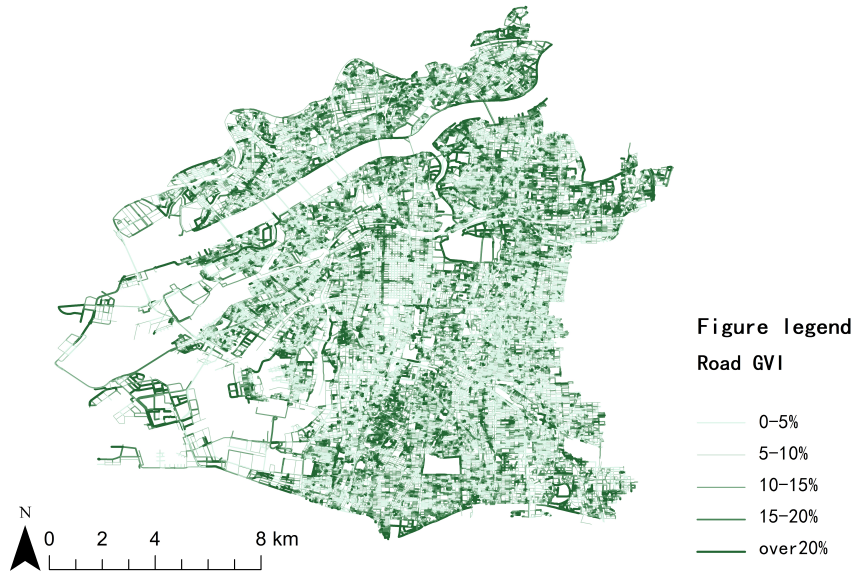
## 4. GVI Best Path Analysis

### 4.1. GVI Best Path by ArcGIS

Firstly, by the cell statistics tool, we can get the raster returned by the corridor analysis tool, the sum of the cost distances (cumulative cost) of the two input cost rasters is calculated for each image location. With this idea, the line graphs of the GVI distribution of Osaka City were exported to raster files according to the satisfaction thresholds of GVI (0~10%, 10~18%, 18~25%, and more than 25%) and assigned resistance values of 200, 150, 100, 50 respectively. The land use data of Osaka City was also assigned with the corresponding resistance values according to the land attributes. Assign a resistance value greater than 200 to all land outside the road in order to make the path travel in the direction of the road. We assigned Nagai Park as the start



(a) The GVI distribution of node map in Osaka City



(b) The GVI distribution of line map in Osaka City.

Figure 7. The node map and line map of GVI distribution in Osaka City.

point and Utsubo Park as the destination as an example. The Nagai Park was used as a source point, therefore two cost accumulation rasters were created. We took the same approach to set Utsubo Park as another source point, the process of creating cost surfaces based on individual image

locations actually occurs at each image location of the input raster, and the total cumulative cost of the path through the image is calculated. However, the result we obtained was a very coarse path band, which had no practical value for the GVI best path analysis, so we decisively abandoned this

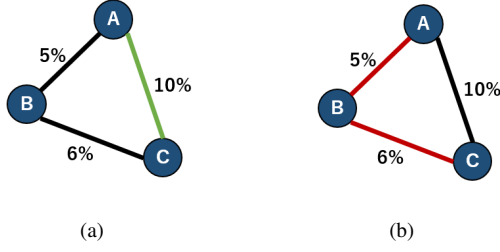


Figure 8. Define the start point is A, final point is C. The value (%) means GVI of each line. (a) The error path (green) by ArcGIS. (b) The correct path (red).

method.

Therefore, we tried a new method to make an attempt at the calculation of the GVI best path in ArcGIS. Geometric network analysis has many applications in calculating the shortest distance between two nodes, such as Dijkstra's Algorithm. We tried to see whether this logic could also be applied to try to calculate the GVI best between two nodes. First, we import the GVI node map and GVI line map of the GVI distribution in Osaka City, and transform them into data set to generate a geometric network. We have the average GVI of each node and set the GVI of the line between two nodes to the average GVI of the two nodes. Because there is no algorithm for the longest path in ArcGIS, we need to adjust the GVI of each line segment to inverse to get the new GVI of this line segment. However, If we take negative values directly, the shortest path problem does not apply (ArcGIS shortest path algorithm requires positive weights between points). We attempted to convert the maximum GVI problem into a shortest path problem by assigning a value of  $(100 - GVI)$  to each line. In this case, we actually need the number of points to ensure that the result obtained using the shortest path algorithm is correct after the  $(100 - GVI)$  transformation. This resulted in the best path being biased towards a path with fewer nodes. This can be seen in the simple dotted line diagram Fig.8.

ArcGIS software is unable to derive the number of points to be passed in the shortest path problem. Similarly, if information on the number of points is not available when finding the shortest path, the correct shortest path is not obtained. Therefore, it is not advisable to convert the maximum GVI path problem directly to a shortest path problem using software because the maximum GVI path does not have the same information about the geometric space, such as the path length, as the shortest path problem. This results in a problem, for instance, in geometric space a long stretch of road, where the GVI value is very low and we have to incorporate information about the number of points in order to make the best GVI path obtained after the  $(100 - GVI)$  transformation of the graph the correct one.

---

**Algorithm 1** Floyd Algorithm using Adjacency Matrix.

---

**Input:** Adjacency Matrix *graph*, number of nodes *N*, the matrix used to store the parent nodes *parents*.

```

for k in Ntimes do
  for i in Ntimes do
    for j in Ntimes do
      if  $graph[i][k] + graph[k][j] < graph[i][j]$  then
         $graph[i][j] = graph[i][k] + graph[k][j]$ 
         $parents[i][j] = parents[k][j]$ 
      end if
    end for
  end for
end for

```

**Output:** a *parents* matrix with the shortest path.

---



---

**Algorithm 2** Get adjacency matrix from adjacency table

---

**Input:** adjacency table (node, node, GVI) file *data*, number of nodes *N*, (N, N)matrix with diagonal elements as 0 and other elements as  $\inf graph$

```

for u, v, c in data do
   $graph[u][v] \leftarrow 0$ 
   $graph[v][u] \leftarrow 0$  {undirected graph}
end for

```

**Output:** adjacency matrix *graph*

---

## 4.2. The GVI Best Path by Adjacency Matrix and Floyd-Warshall Algorithm

In order to calculate the best GVI path between any two points, we decided to use the adjacency matrix as the starting point and use Floyd-Warshall Algorithm (see Algorithms 1) to calculate the best GVI path. The adjacency relationship between points and lines can be obtained from ArcGIS. The adjacency table of all points and lines can be obtained by transformation, and the weights are the transformed GVI values  $(100 - GVI)$  as well as the undirected graph is used to represent the adjacency matrix. Since the adjacency matrix contains information about the number of points, we can use  $(100 - GVI)$  to convert the problem into a shortest path problem without any concern. As shown in Algorithm 2, with the adjacency matrix, Floyd-Warshall Algorithm can derive a list of node arrangements for the best path, and finally we can represent the best GVI path on the graph. It is important to mention that we can obtain the adjacency matrix of the region as a whole after a long time, for instance, if we use a region containing about 5000 points for the adjacency matrix generation operation, it takes nearly three hours to achieve this process. Once we have the adjacency matrix, specifying the start and destination can promptly lead to an GVI best path and import the basic information into ArcGIS to visualize the path. We choose Nagai Park as the start point, drive north, and select



Figure 9. The GVI best path from Nagai Park to Utsubo Park and street view examples by adjacency matrix and Floyd-Warshall Algorithm.

Utsubo Park as the destination, and the best GVI path obtained according to the proposed method is shown in Fig.9.

#### 4.3. A More Realistic Attempt

The  $GVI_{avg}$  of each line is used as a measure to calculate the GVI best path for any location. However, in a continuous landscape of real life, human eye mainly observes the landscape in the direction of travel, and the average GVI of two nodes is not used to replace the GVI value of the line. Therefore, a more accurate calculation method for the GVI best path should be proposed to select the direction of maximum GVI at each intersection, and finally the GVI of the overall travel direction of the route gets the maximum value. The Imazu Park is an ideal area to test this idea, because it is almost a square area, while each node faces east, west, north and south horizontally and vertically as well as the street view image we intercepted can be a well-represented view of the tourists' direction of travel.

In the example of the Imazu Park in Osaka City, we collected street view images from the angle of the road and processed them to obtain the GVI value of each direction of the intersection, following the method of collecting and analyzing street view images in Osaka City. We obtained  $0^\circ$ ,  $90^\circ$ ,  $180^\circ$ , and  $270^\circ$  street view images of each intersection. With respect to the treatment of the adjacency matrix, we adopted a bi-directional directed graph instead of the previous undirected graph to include more information of weights. The best path was calculated based on the street direction GVI as shown in Fig.10.

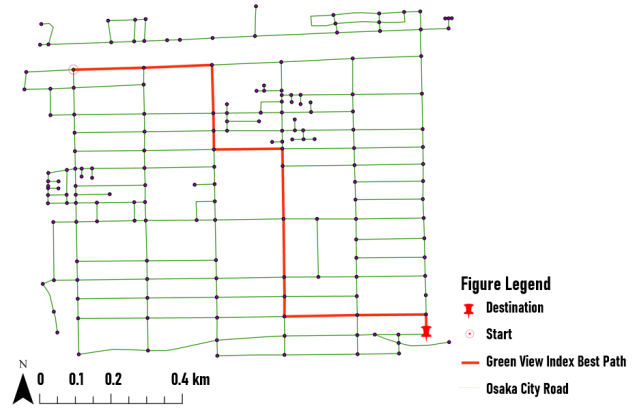


Figure 10. Calculation of the GVI best path based on the GVI facing the street direction.

## 5. Discussion and Result

### 5.1. The GVI Analysis of Osaka City

In the part of GVI analysis in this paper, there are 37,622 intersections with an average GVI between 0~10% of the 49,770 intersections in Osaka City overall, accounting for 75.59% of the total; there are 7,914 intersections with an average GVI between 10~18%, representing 15.9% of the total; 2,629 intersections with an average GVI between 18~25%, which represents 5.28% of the total; 1,605 inter-



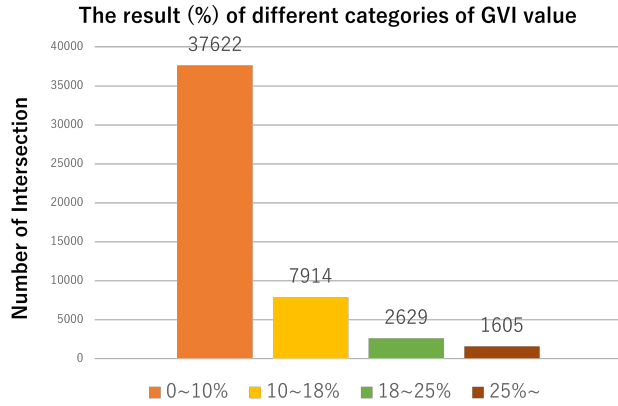


Figure 11. The result of different categories of GVI value in Osaka City.

sections (3.22% of the total) have an average GVI of 25%~. From the result of statistics based on HRNet-OCR, it can be seen that Osaka City has a low level of GVI value and Low satisfaction based on the percentage over 25% of GVI (see Fig.11). Since we selected to use the "drive" method for the road sections, we did not capture usable street view images and calculate the corresponding GVI values for the sections that were not passable by vehicles but were passable by pedestrians on foot. The most obvious areas, such as Osaka Castle and Nagai Park, are not clearly represented on the GVI distribution map (see Fig.12).

Based on the distribution data of the GVI in Osaka City, the results of calculating the GVI best path can be derived. The following summarizes the results of different three methods: GVI best path by ArcGIS, adjacency matrix and Floyd-Warshall Algorithm, as well as the more realistic attempt.

## 5.2. The GVI Best Path of Osaka City

The threshold output produced in the reference corridor analysis can be thought of as a least-cost corridor for image elements, rather than a least-cost path. From Nagai Park to Utsubo Park, it is the path zone, not the specific route, that is planned. We can only obtain a general path zone, which is not applicable in actual tourist route due to the lack of sufficient detail and the nature of travel along the path. However, we are inspired by the fact that this path zone allows us to roughly derive the direction of travel of the best GVI path, and it is a direction that is worth considering and practising whether this approximate direction of travel can be applied to optimal GVI path analysis when operations such as the path adjacency matrix are too computationally intensive. For the second method, the geometric network analysis method, taking the path from Nagai Park to Utsubo Park as an example, the geometric network analysis method is applicable to design multiple stopping nodes,

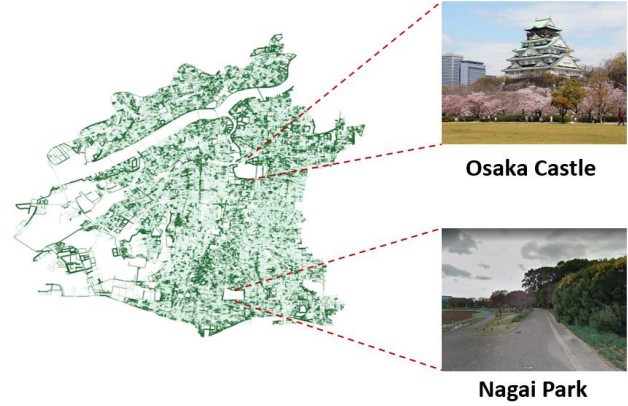


Figure 12. Areas not captured in the GVI distribution map: Osaka Castle and Nagai Park.

but this method is not feasible as we can not actually obtain the correct GVI path due to the lack of the important information of the number of points through which the path passes. However, this method, known as network analysis, can be used not only for the planning of tourist routes in the area, but also for the evaluation of neighborhood landscapes and the evaluation of business values in the area.

We made good use of the point-line relationships derived from ArcGIS and generated the corresponding adjacency matrix. Floyd-Warshall Algorithm is a feasible method and we finally get the correct GVI best path. This method can be used in urban tourism route design, marathon race route design, and other situations where urban landscape needs to be displayed. However, due to its long computation time, we are considering other methods to save computation time and improve efficiency. We have verified the correctness of the GVI best path and the most intuitive way to gain an intuitive understanding is by comparing the GVI values of neighbouring roads with it. The adjacency matrix allows the coordinates and GVI values of the points through which the path passes to be returned. As shown in Fig.9, we randomly selected street images of several inflection points and aligned them. This best GVI path passed through a total of 120 points (included start and destination), and the average GVI of this path was 7.47%.

For the realistic calculation method, the GVI best path is calculated based on the directional GVI values. Take the example of the northwest node to the southeast node of Imazu Park in Osaka City. We can obtain the GVI best path utilising the traditional method of converting the best GVI path problem into a shortest path problem using ArcGIS software. This area, because of its square shape and the coincidental direction of the roads (basically the roads are facing due north, south, west and east.) , there is no limit to the number of nodes, so the correct best GVI path

can be obtained with conventional ArcGIS. We have studied this area using a generic adjacency matrix and the Floyd-Warshall Algorithm. The GVI assignment of the roads was performed using a different strategy, i.e. a street view of each point facing the street was calculated as a GVI assignment to the lines, instead of the previous assignment of each line by the average of the nodes connected to it. Because the detailed GVI values are calculated for the different directions of each node, we can obtain a more realistic GVI best path, as in a real world implementation. However, this method is quite cumbersome in GVI statistics. As the roads in Imazu Park intersect each other vertically, it is possible to set up the download of street view images at 0°, 90°, 180° and 270°. With regard to the part of the adjacency matrix, instead of undirected maps, we use directed maps with different directions to generate the adjacency matrix, so that there are two directions with different weights for each line, and accordingly, the cost of the calculation will be increased. This method of implementing the best GVI paths to match realistic scenarios is not easily achievable due to its strict constraints and high computational cost to calculate street view images of road directions and compute paths in areas with complicated and uncertain road intersection angles. This method could be better improved and generalised if there exist an optional parameter on the road angle of the street intersections in the investigated city. In addition, In order to fill in the gaps of non-drivable roads, in the future we will collect street view images in a walkable way to get improved and more complete results.

## 6. Conclusion

In this paper, we implement a semantic segmentation network in deep learning to analyse the Green View Index in Osaka City. We implement the GVI analysis in a large scale as well as get reasonable results and visualize them with feasible methods. After obtaining the basic GVI distribution of Osaka city, we proposed innovative generic approach to calculate the GVI best path and verified it more carefully and accurately in a limited area. Not only did we implement the GVI best path by street view images, filling a gap in this application, but we also demonstrated the feasibility of this research, which allows us to guide better lifestyles through street views.

## References

- [1] Sjerp De Vries, Sonja Me Van Dillen, Peter P Groenewegen, and Peter Spreeuwenberg. Streetscape greenery and health: Stress, social cohesion and physical activity as mediators. *Social science & medicine*, 94:26–33, 2013.
- [2] E Gregory McPherson, James R Simpson, Qingfu Xiao, and Chunxia Wu. Million trees los angeles canopy cover and benefit assessment. *Landscape and Urban Planning*, 99(1):40–50, 2011.
- [3] Timothy Van Renterghem and Dick Botteldooren. View on outdoor vegetation reduces noise annoyance for dwellers near busy roads. *Landscape and urban planning*, 148:203–215, 2016.
- [4] Francesco Ferrini, Alessio Fini, Jacopo Mori, and Antonella Gori. Role of vegetation as a mitigating factor in the urban context. *Sustainability*, 12(10):4247, 2020.
- [5] Lun Liu, Elisabete A Silva, Chunyang Wu, and Hui Wang. A machine learning-based method for the large-scale evaluation of the qualities of the urban environment. *Computers, environment and urban systems*, 65:113–125, 2017.
- [6] Biao Zhang, Ji-xi Gao, Yang Yang, et al. The cooling effect of urban green spaces as a contribution to energy-saving and emission-reduction: A case study in beijing, china. *Building and environment*, 76:37–43, 2014.
- [7] Xiaojiang Li, Chuanrong Zhang, Weidong Li, Robert Ricard, Qingyan Meng, and Weixing Zhang. Assessing street-level urban greenery using google street view and a modified green view index. *Urban Forestry & Urban Greening*, 14(3):675–685, 2015.
- [8] Rencai Dong, Yonglin Zhang, and Jingzhu Zhao. How green are the streets within the sixth ring road of beijing? an analysis based on tencent street view pictures and the green view index. *International journal of environmental research and public health*, 15(7):1367, 2018.
- [9] Jun Yang, Linsen Zhao, Joe McBride, and Peng Gong. Can you see green? assessing the visibility of urban forests in cities. *Landscape and Urban Planning*, 91(2):97–104, 2009.
- [10] Nanqi Ye, Bowen Wang, Michihiro Kita, Ming Xie, and Wenyue Cai. Urban commerce distribution analysis based on street view and deep learning. *IEEE Access*, 7:162841–162849, 2019.
- [11] Bowen Wang, Liangzhi Li, Yuta Nakashima, Ryo Kawasaki, Hajime Nagahara, and Yasushi Yagi. Noisy-lstm: Improving temporal awareness for video semantic segmentation. *IEEE Access*, 9:46810–46820, 2021.
- [12] Ming Tong, Jiangfeng She, Junzhong Tan, Mengyao Li, Rongcun Ge, and Yiyuan Gao. Evaluating street greenery by multiple indicators using street-level imagery and satellite images: A case study in nanjing, china. *Forests*, 11(12):1347, 2020.
- [13] Ryuhei Uehara and Yushi Uno. Efficient algorithms for the longest path problem. In *International symposium on algorithms and computation*, pages 871–883. Springer, 2004.
- [14] Kairanbay Magzhan and Hajar Mat Jani. A review and evaluations of shortest path algorithms. *International journal of scientific & technology research*, 2(6):99–104, 2013.
- [15] Yuhui Yuan, Xiaokang Chen, Xilin Chen, and Jingdong Wang. Segmentation transformer: Object-contextual representations for semantic segmentation. *arXiv preprint arXiv:1909.11065*, 2019.
- [16] Xiaojiang Li, Chuanrong Zhang, and Weidong Li. Does the visibility of greenery increase perceived safety in urban areas? evidence from the place pulse 1.0 dataset. *ISPRS*

- International Journal of Geo-Information*, 4(3):1166–1183, 2015.
- [17] Jian Kang, Marco Körner, Yuanyuan Wang, Hannes Taubenböck, and Xiao Xiang Zhu. Building instance classification using street view images. *ISPRS journal of photogrammetry and remote sensing*, 145:44–59, 2018.
  - [18] Alfredo Canziani, Adam Paszke, and Eugenio Culurciello. An analysis of deep neural network models for practical applications. *arXiv preprint arXiv:1605.07678*, 2016.
  - [19] Hengshuang Zhao, Jianping Shi, Xiaojuan Qi, Xiaogang Wang, and Jiaya Jia. Pyramid scene parsing network. In *Proceedings of the IEEE conference on computer vision and pattern recognition*, pages 2881–2890, 2017.
  - [20] Xinxiang Zhang, Dinesh Rajan, and Brett Story. Concrete crack detection using context-aware deep semantic segmentation network. *Computer-Aided Civil and Infrastructure Engineering*, 34(11):951–971, 2019.
  - [21] Yu Gordienko, Peng Gang, Jiang Hui, Wei Zeng, Yu Kochura, Oleg Alienin, Oleksandr Rokovyi, and Sergii Stirenko. Deep learning with lung segmentation and bone shadow exclusion techniques for chest x-ray analysis of lung cancer. In *International Conference on Computer Science, Engineering and Education Applications*, pages 638–647. Springer, 2018.
  - [22] Mennatullah Siam, Sara Elkerdawy, Martin Jagersand, and Senthil Yogamani. Deep semantic segmentation for automated driving: Taxonomy, roadmap and challenges. In *2017 IEEE 20th international conference on intelligent transportation systems (ITSC)*, pages 1–8. IEEE, 2017.
  - [23] Olaf Ronneberger, Philipp Fischer, and Thomas Brox. U-net: Convolutional networks for biomedical image segmentation. In *International Conference on Medical image computing and computer-assisted intervention*, pages 234–241. Springer, 2015.
  - [24] Vijay Badrinarayanan, Alex Kendall, and Roberto Cipolla. Segnet: A deep convolutional encoder-decoder architecture for image segmentation. *IEEE transactions on pattern analysis and machine intelligence*, 39(12):2481–2495, 2017.
  - [25] Liang-Chieh Chen, Yukun Zhu, George Papandreou, Florian Schroff, and Hartwig Adam. Encoder-decoder with atrous separable convolution for semantic image segmentation. In *Proceedings of the European conference on computer vision (ECCV)*, pages 801–818, 2018.
  - [26] Marius Cordts, Mohamed Omran, Sebastian Ramos, Timo Rehfeld, Markus Enzweiler, Rodrigo Benenson, Uwe Franke, Stefan Roth, and Bernt Schiele. The cityscapes dataset for semantic urban scene understanding. In *Proceedings of the IEEE conference on computer vision and pattern recognition*, pages 3213–3223, 2016.
  - [27] Ke Sun, Bin Xiao, Dong Liu, and Jingdong Wang. Deep high-resolution representation learning for human pose estimation. In *CVPR*, 2019.
  - [28] Xiaojiang Li. Examining the spatial distribution and temporal change of the green view index in new york city using google street view images and deep learning. *Environment and Planning B: Urban Analytics and City Science*, 48(7):2039–2054, 2021.
  - [29] Yusuke Kumakoshi, Sau Yee Chan, Hideki Koizumi, Xiaojiang Li, and Yuji Yoshimura. Standardized green view index and quantification of different metrics of urban green vegetation. *Sustainability*, 12(18):7434, 2020.
  - [30] Mehmet Cetin. Using gis analysis to assess urban green space in terms of accessibility: case study in kutahya. *International Journal of Sustainable Development & World Ecology*, 22(5):420–424, 2015.
  - [31] Yoshiki Yamagata, Daisuke Murakami, Takahiro Yoshida, Hajime Seya, and Sho Kuroda. Value of urban views in a bay city: Hedonic analysis with the spatial multilevel additive regression (smar) model. *Landscape and Urban Planning*, 151:89–102, 2016.
  - [32] Joachim Rußig and Julian Bruns. Reducing individual heat stress through path planning. *GI-Forum*, 1:327–340, 2017.
  - [33] Joose Helle, Age Poom, Elias S Willberg, and Tuuli Toivonen. The green paths route planning software for exposure-optimised travel. 2021.
  - [34] Dengkai Huang, Bin Jiang, and Lei Yuan. Analyzing the effects of nature exposure on perceived satisfaction with running routes: An activity path-based measure approach. *Urban Forestry & Urban Greening*, page 127480, 2022.
  - [35] Tessio Novack, Zhiyong Wang, and Alexander Zipf. A system for generating customized pleasant pedestrian routes based on openstreetmap data. *Sensors*, 18(11):3794, 2018.
  - [36] Geoff Boeing. Osmnx: New methods for acquiring, constructing, analyzing, and visualizing complex street networks. *Computers, Environment and Urban Systems*, 65:126–139, 2017.
  - [37] Yuhui Yuan, Xilin Chen, and Jingdong Wang. Object-contextual representations for semantic segmentation. In *European conference on computer vision*, pages 173–190. Springer, 2020.
  - [38] Ashish Vaswani, Noam Shazeer, Niki Parmar, Jakob Uszkoreit, Llion Jones, Aidan N. Gomez, Lukasz Kaiser, and Illia Polosukhin. Attention is all you need, 2017.